

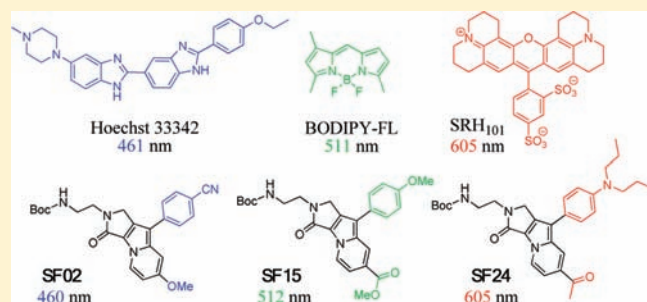
Emission Wavelength Prediction of a Full-Color-Tunable Fluorescent Core Skeleton, 9-Aryl-1,2-dihydropyrrolo[3,4-*b*]indolizin-3-one

Eunha Kim,[†] Minseob Koh,[†] Byung Joon Lim,[†] and Seung Bum Park^{*,†,‡}

[†]Department of Chemistry and [‡]Department of Biophysics and Chemical Biology, Seoul National University, Seoul 151-747, Korea

S Supporting Information

ABSTRACT: In this paper we report on a novel fluorescent core skeleton, 9-aryl-1,2-dihydropyrrolo[3,4-*b*]indolizin-3-one, which we named Seoul-Fluor, having tunable and predictable photophysical properties. Using a concise and practical one-pot synthetic procedure, a 68-member library of new fluorescent compounds was synthesized with diverse substituents. In Seoul-Fluor, the electronic characteristics of the substituents, as well as their positional changes, have a close correlation with their photophysical properties. The systematic perturbation of electronic densities on the specific positions of Seoul-Fluor, guided with the Hammett constant, allows emission wavelength tunability covering the full color range. On the basis of these observations and a computational analysis, we extracted a simple first-order correlation of photophysical properties with the theoretical calculation and accurately predicted the emission wavelength of Seoul-Fluors through the rational design. In this study, we clearly demonstrate that Seoul-Fluor can provide a powerful gateway for the generation of desired fluorescent probes without the need for a tiresome synthesis and trial-and-error process.



INTRODUCTION

Due to the favorable properties of fluorescent probes, such as excellent sensitivity, low cost, a large linear range of analysis, and ease of handling,¹ they have been used extensively as research tools in biological science² and clinical diagnosis and drug discovery.³ Fluorescent materials also have received considerable attention due to their potential applications as organic light-emitting diodes (OLEDs).⁴ For expansion of fluorescence-based applications, particularly for multiplexing capability in biological applications, the scientific community has focused on controlling the emission wavelength of fluorescent probes.⁵ Despite the popularity of organic fluorophores, the number of core skeletons possessing emission wavelength tunability⁶ is quite limited, and a rational design of a fluorescent probe with desirable photophysical properties is still far from being achieved. BODIPY and cyanine dyes are the only known organic fluorophores with correlation between structures and their photophysical properties.⁷ However, their tunability was discovered by extensive trial-and-error-based research, and their molecular structure must be significantly changed to tune the emission wavelength without predictability.

A well-known group of fluorescent probes with tunable and predictable emission wavelengths is made up of semiconductor nanocrystals, known as quantum dots (QDs),⁸ which are generally composed of heavy metals such as CdSe and CdTe.^{9–11} The fascinating modulation characteristics of QDs, which can emit any color from fundamentally equal starting material through a simple adjustment in their radius and shape,¹² have brought them into the spotlight for potential application as powerful fluorescent probes in the biological and medical

sciences in recent years.^{13,14} However, despite their recent improvements, QDs are still not completely suitable for biological applications due to their innate toxicity.¹⁵

Despite the high demand for the development of a new tunable organic fluorophore with predictable photophysical properties,¹⁶ the prediction of such photophysical properties is currently impractical. The fluorescent emission wavelength and quantum yield (QY) are nearly impossible to predict on the basis of the structural modification of a fluorescent core skeleton with a given functional group, due to the complexity of underlying photophysical phenomena in organic molecules.¹⁷ Therefore, the discovery of new fluorescence probes has been empirically pursued with limited synthetic flexibility. Fortunately, the birth of combinatorial chemistry in the early 1990s has ensured that these previous limitations can be overcome, particularly those regarding the difficulties in the rational design of organic fluorophores with synthetic flexibility.^{5,18} Since an initial effort beginning in 2001,¹⁹ the low efficiency in the structural modifications of existing fluorescent core skeletons has been somewhat addressed through the application of combinatorial chemistry for the development of new fluorescent compounds.²⁰ Although many researchers have recently utilized sophisticated combinatorial techniques to reveal new fluorescent probes with various emission wavelengths, novel fluorescent skeletons with tunable and predictable photophysical properties are still rare. Here, we report the discovery and systematic study of a full-color-tunable

Received: December 1, 2010

Published: April 12, 2011

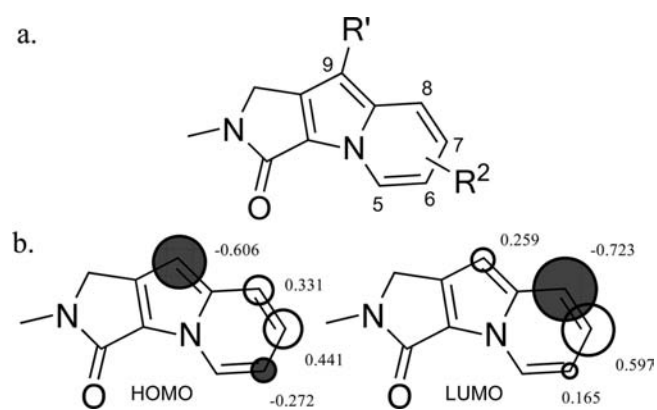


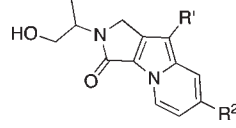
Figure 1. Structural and computational study of a fluorescent core skeleton. (a) Structure of the fluorescent core skeleton. (b) Schematic figure of the atomic coefficients of the HOMO and LUMO. The sizes and colors of the circles indicate the π -electron density and phase difference of the orbitals, respectively.

fluorescent core skeleton, 9-aryl-1,2-dihydropyrrolo[3,4-*b*]indolizin-3-one, with a predictable emission wavelength; we name it Seoul-Fluor.²¹

RESULTS AND DISCUSSION

In Silico Analysis of Molecular Orbitals on the Fluorescent Core Skeleton. During a recent attempt to develop a synthetic pathway for a new core skeleton using diversity-oriented synthesis,²² we reported the discovery of a novel fluorescent molecular framework.²¹ This fluorescent core skeleton was originally designed with an excellent substituent-pending potential. Hence, using a combinatorial approach, we envisioned to extract the relationship of substituents with the photophysical properties through a systematic analysis of a series of fluorescent compounds with an identical core skeleton. Prior to the construction of these fluorescent compounds, we pursued a rational design through theoretical calculation to identify the ideal position of the substituent to maximize the perturbation in their electronic characters for the changes on photophysical properties. Using density functional theory (DFT) calculations with the generalized gradient corrected Perdew–Burke–Ernzerhof (GGA-PBE) functional and the double numerical polarized (DNP) basis set,²³ the atomic coefficients of the highest occupied molecular orbital (HOMO) and the lowest unoccupied molecular orbital (LUMO) in the fluorescent core skeleton were calculated (Figure 1). First, there is a significant size difference between the HOMO and LUMO lobes at the C-9 position, where the lobe size of the LUMO is considerably smaller than that of the HOMO, leading to an expected destabilization of the HOMO through the introduction of electron-rich substituents. Hence, the energy gap between the HOMO and LUMO is expected to decrease owing to the introduction of an electron-donating group (EDG) at the C-9 position.²⁴ However, the relationship between the photophysical properties and the R² group is less clear than the relationship between the photophysical properties and the R' group. Nevertheless, for the R² group, the LUMO lobe is larger than the HOMO lobe at the C-7 and C-8 positions. Therefore, we hypothesize that the energy gap will decrease with the introduction of an electron-withdrawing group (EWG) in regioisomeric positions of the R² group, owing to the stabilization of the LUMO.

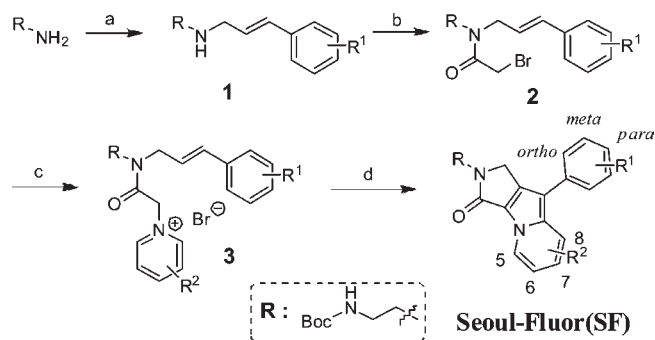
Table 1. Initial Analysis of the Relationship between Structural and Photophysical Properties Based on Our Original Collection of Fluorescent Compounds



compd	R'	R ²	λ_{abs}^a	λ_{em}^b	$\Delta(\text{eV})^c$	Φ_{F}^d
A1	methyl	hydrogen	326	434	3.83	0.41
A2	methyl	methoxy				
A3	methyl	phenyl	342	433	3.29	0.19
A4	methyl	nitrile	349	460	3.34	0.76
A5	methyl	acetyl	396	471	3.14	0.82
B1	phenyl	hydrogen	298	420	3.48	0.57
B2	phenyl	methoxy	320	481	3.28	0.27
B3	phenyl	phenyl	388	490	3.19	0.83
B4	phenyl	nitrile	350	497	3.18	0.65
B5	phenyl	acetyl	403	507	2.98	0.74
C1	2-methoxyphenyl	hydrogen	320	461	3.50	0.37
C2	2-methoxyphenyl	methoxy	323	465	3.29	0.26
C3	2-methoxyphenyl	phenyl	391	489	3.18	0.69
C4	2-methoxyphenyl	nitrile	381	493	3.15	0.55
C5	2-methoxyphenyl	acetyl	404	508	2.95	0.71
D1	2-thiophenyl	hydrogen	322	481	3.26	0.08
D2	2-thiophenyl	methoxy	302	500	3.12	0.03
D3	2-thiophenyl	phenyl	398	515	3.02	0.11
D4	2-thiophenyl	nitrile	283	529	2.89	0.15
D5	2-thiophenyl	acetyl	349	540	2.70	0.35
E1	4-(dimethylamino)phenyl	hydrogen	298	495	3.23	0.10
E2	4-(dimethylamino)phenyl	methoxy	311	480	3.11	0.03
E3	4-(dimethylamino)phenyl	phenyl	428	530	2.88	0.21
E4	4-(dimethylamino)phenyl	nitrile	403	509	2.78	0.13
E5	4-(dimethylamino)phenyl	acetyl	440	613	2.56	0.15

^a Only the largest absorption maxima are shown. ^b Excited at the maximum absorption wavelength. ^c Calculated value of the energy gap between the S₀ and S₁ states (see the Supporting Information). ^d Absolute fluorescence quantum yield. Absolute quantum yields of known fluorescent dyes at various wavelengths were measured to confirm the reliability of the system [anthracene, $\Phi_{\text{F}} = 0.27$ (reported 0.27);²⁵ fluorescein, $\Phi_{\text{F}} = 0.76$ (reported 0.79);²⁶ cresyl violet, $\Phi_{\text{F}} = 0.48$ (reported 0.54)²⁷]. The A2 compound was not feasible in this study.

Preanalysis of Substituent Effects on the Photophysical Properties of Seoul-Fluor Based on Our Original Collection of Fluorescent Compounds. Using a combination of five α,β -unsaturated aldehydes and five pyridines with various electronic properties, we previously constructed 24 discrete fluorescent compounds using a single-core skeleton, 1,2-dihydropyrrolo[3,4-*b*]indolizin-3-one.²¹ For simplicity and efficiency of the synthetic procedure, in the beginning of this study, we focused on the relationship of the photophysical properties with the R² substituents at the C-7 position rather than at the other available positions. Hence, *para*-substituted pyridines were used initially to introduce various substituents as the R² group at the C-7 position. The fluorescent emission spectra listed in Table 1 demonstrate the novelty of this full-color-tunable fluorescent core skeleton. Through the introduction of various substituents at the R' and R² positions on a single-core skeleton, we achieved a collection of novel fluorescent compounds with a full coverage of emission wavelengths in the visible region. It is remarkable that simple changes of substituents at only two variation points of the fluorescent core skeleton result in dramatic changes of their emission wavelengths. A direct comparison between the electronic properties of the R' substituents and the photophysical

Scheme 1. Synthetic Scheme of 9-Aryl-1,2-dihydropyrrolo[3,4-*b*]indolizin-3-one^a

^a Reagents and conditions: (a) α,β -unsaturated aldehydes, AcOH, Na₂SO₄, DCM, rt; then NaBH₄, MeOH, 0 °C; (b) bromoacetyl bromide, TEA, DCM, -78 °C; (c) pyridines; (d) DBU, toluene and DCM (1:1, v/v); then DDQ.

properties of Seoul-Fluor clarifies its tunable emission wavelength. Consistent with our initial assumption, the calculated energy gap between the S₀ and S₁ states decreased with intensifying EDG at the R' position or EWG at the R² position. An enhanced electron richness at the R' position results in a bathochromic shift of the emission wavelength: Substituent changes of methyl (A5) to phenyl (B5), 2-methoxyphenyl (C5), 2-thiophenyl (D5), and 4-(dimethylamino)phenyl (E5) result in red shifts (or bathochromic shifts) from 471 to 507, 508, 540, and 613 nm, respectively, in the emission wavelength. Likewise, at the R² position, substituent changes of hydrogen (B1) to methoxy (B2), phenyl (B3), nitrile (B4), and acetyl (B5) cause bathochromic emission wavelength shifts from 420 to 481, 490, 497, and 507 nm, respectively.

General Synthetic Scheme for the Fluorescent Core Skeleton. After the analysis of our computational study and convenient structure–photophysical property relationship studies based on the original set of fluorophores, we finalized the fluorescent core skeleton as 9-aryl-1,2-dihydropyrrolo[3,4-*b*]indolizin-3-one and named it Seoul-Fluor (SF). We also optimized the synthetic pathway to construct a new fluorescent compound library, with the potential for further diversification using combinatorial chemistry. As shown in Scheme 1, we first introduced the R¹ group via reductive amination of cinnamaldehyde derivatives with primary amine. The resulting secondary amines **1** were acylated with bromoacetyl bromide, which was followed by the nucleophilic substitution of alkyl bromide **2** with pyridine analogues, where the R² groups can be introduced. The crude pyridinium salts **3** were then subjected to an intramolecular 1,3-dipolar cycloaddition of olefin with azomethine ylide in situ generated through DBU treatment of **3**. The final DDQ-assisted oxidative aromatization transformed the resulting nonfluorescent tricyclic adduct into the fluorescent core skeleton, 9-aryl-1,2-dihydropyrrolo[3,4-*b*]indolizin-3-one, in a one-pot fashion.

Systematic Evaluation of Substituent Effects on the Photophysical Properties of Seoul-Fluor. As mentioned previously, the electronic character of the R¹ and R² groups may be important in determining the photophysical properties of Seoul-Fluor. On the basis of our original assumption, we hypothesized that an evaluation of the relationship between their structures and photophysical properties can be possible via the systematic perturbation of electronic characters at the R¹ and R² positions. To provide a guideline for an efficient selection of substituents

Table 2. Electronic Effect of Substituents on the Relationship between the Structural and Photophysical Properties of Seoul-Fluor

compd	R ¹	σ_p^a	R ²	λ_{abs}^b	$\Delta(\text{eV})^c$	λ_{em}^d	Φ_F^e
SF01	CN	0.66	CH ₃	344	3.29	445	0.67
SF02	CN	0.66	OCH ₃	344	3.23	460	0.58
SF03	CN	0.66	CO ₂ CH ₃	394	3.07	487	0.99
SF04	CN	0.66	COCH ₃	407	2.96	494	0.99
SF05	Br	0.23	CH ₃	318	3.48	462	0.33
SF06	Br	0.23	OCH ₃	325	3.31	476	0.30
SF07	Br	0.23	CO ₂ CH ₃	393	3.20	492	0.90
SF08	Br	0.23	COCH ₃	405	2.98	502	0.90
SF09	CH ₃	-0.17	CH ₃	344	3.47	471	0.63
SF10	CH ₃	-0.17	OCH ₃	337	3.25	485	0.24
SF11	CH ₃	-0.17	CO ₂ CH ₃	396	3.16	498	0.88
SF12	CH ₃	-0.17	COCH ₃	408	2.93	509	0.80
SF13	OCH ₃	-0.27	CH ₃	345	3.42	482	0.41
SF14	OCH ₃	-0.27	OCH ₃		3.22		
SF15	OCH ₃	-0.27	CO ₂ CH ₃	400	2.99	512	0.68
SF16	OCH ₃	-0.27	COCH ₃	412	2.84	526	0.69
SF17	N(Ph) ₂	-0.22	CH ₃	332	3.25	497	0.22
SF18	N(Ph) ₂	-0.22	OCH ₃		3.08		
SF19	N(Ph) ₂	-0.22	CO ₂ CH ₃	412	2.70	554	0.42
SF20	N(Ph) ₂	-0.22	COCH ₃	428	2.49	579	0.40
SF21	N(Pr) ₂	-0.93	CH ₃		3.14		
SF22	N(Pr) ₂	-0.93	OCH ₃		3.02		
SF23	N(Pr) ₂	-0.93	CO ₂ CH ₃	429	2.69	586	0.18
SF24	N(Pr) ₂	-0.93	COCH ₃	445	2.49	605	0.20

^a σ_p is the parameter for the Hammett constant of the *para*-position from ref 28. ^b Only the largest absorption maxima are shown. ^c Calculated value of the energy gap between the S₀ and S₁ states (see the Supporting Information). ^d Excited at the maximum absorption wavelength. ^e Absolute fluorescence quantum yield. Absolute quantum yields of known fluorescent dyes at various wavelengths were measured to confirm the reliability of the system [anthracene, $\Phi_F = 0.27$ (reported 0.27);²⁵ fluorescein, $\Phi_F = 0.76$ (reported 0.79);²⁶ cresyl violet, $\Phi_F = 0.48$ (reported 0.54)²⁷]. SF14, SF18, SF21, and SF22 compounds were not feasible in this study.

with various electronic characters, we introduced the Hammett substituent constant (σ)²⁸ as a numerical value for the quantification of the electronic effects of a substituent. We also synthesized a series of Seoul-Fluors using various substituents with a broad range of σ to confirm our original assumption that the electronic effect on the photophysical properties can also be extended to different substituents. On the basis of our *in silico* analysis, we first focused on Seoul-Fluor with R¹ substituents at the *para*-position on the phenyl moiety and R² substituents at the C-7 position to clarify the relationship between the structural and photophysical properties. As shown in Table 2, substituents with a wide range of σ_p (Hammett constant for the *para*-position of the phenyl group), from the highest (nitrile) to lowest (dipropylamine) value, were selected at the R¹ position. Compared to its less pronounced correlation with the absorption wavelength, the Hammett substituent constant σ_p of the R¹ group had a significant inverse correlation with the emission wavelength of Seoul-Fluor. For example, with a fixed R² substituent such as acetyl, a

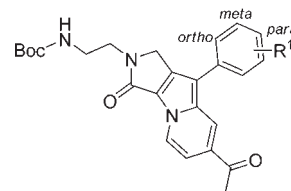
decrease in the Hammett substituent constant from CN (SF04, $\sigma_p = 0.66$) to Br (SF08, 0.23), Me (SF12, -0.17), OMe (SF16, -0.27), and NPr_2 (SF24, -0.93) caused bathochromic emission wavelength shifts from 494 to 502, 509, 523, and 605 nm, respectively. In other words, the electron richness at the R^1 position can directly affect the emission wavelength. Therefore, an adjustment of the electron density of a fluorophore through the introduction of an electron-donating or electron-withdrawing group at the R^1 position can tune the emission wavelength of Seoul-Fluor, which is consistent with our original assumption.

This bathochromic shift in the emission wavelength along with the electron richness of the *para*-positioned R^1 substituents was consistently observed throughout the four different R^2 substituents, which included electron-donating (methoxy, methyl) and electron-withdrawing (ester, acetyl) groups. We also found that the electronic character of the R^2 substituents affects the emission wavelength: the increase in electron-withdrawing ability at the R^2 position from a mild EDG to a strong EWG causes a bathochromic shift of the emission wavelength. For instance, substituent changes from methyl (SF01) to methoxy (SF02), ester (SF03), and acetyl (SF04) caused bathochromic emission wavelength shifts from 445 to 460, 487, and 494 nm, respectively, using a fixed R^1 substituent such as CN. Although the Hammett substituent constant of an indolizine ring at the C-7 position is somewhat ambiguous and it is not clear whether methyl ($\sigma_p = -0.17$, $\sigma_m = -0.07$) in an indolizine ring is a stronger electron-donating group than methoxy ($\sigma_p = -0.27$, $\sigma_m = 0.12$), it is generally observed that an electron deficiency at the R^2 position triggers a bathochromic shift of the emission wavelength in Seoul-Fluor.

It is noteworthy that a full-visible-color emission wavelength was achieved in the Seoul-Fluor single fluorescent core skeleton simply by fine-tuning the electronic characters at the R^1 and R^2 positions: substituent changes of nitrile ($\sigma_p = 0.66$) and methyl ($\sigma_p = -0.17$) (SF01) to dipropylamino ($\sigma_p = -0.93$) and acetyl ($\sigma_p = 0.50$) (SF24) at these positions can also result in a 160 nm bathochromic shift in an identical fluorescent core skeleton.

Positional Effect of R^1 Substituents on the Photophysical Properties of Seoul-Fluor. So far, we have demonstrated that the electron richness of substituents at the R^1 position has a direct correlation with the emission wavelength of Seoul-Fluor. Hence, we focused on our next area of interest, i.e., whether Seoul-Fluor might have a different emission wavelength depending on a substituent's regioisomeric position. To study the positional effect of substituents on the photophysical properties of Seoul-Fluor, we synthesized a series of fluorescent compounds using regioisomeric cinnamaldehyde derivatives for an introduction of various R^1 groups on the *ortho*-, *meta*-, and *para*-positions of Seoul-Fluor. As shown in Table 3, with an acetyl moiety as a fixed R^2 group at the C-7 position, we observed a slight bathochromic shift of the emission wavelength upon a positional shift of the R^1 substituents from *ortho* to *meta* and *para* when R^1 is nitrile, bromo, and methoxy. However, this observation was not consistent in the case of the dimethylamino group at the R^1 substituent. This puzzling phenomenon revealed some meaningful information once we converted those data into a scatter plot of emission wavelength for individual positional regioisomers of Seoul-Fluor. As shown in Figure 2a, we observed drastic changes in the emission wavelength at the *ortho*- and *para*-positions upon changes in the electronic characters of the substituents, but there were marginal changes at the *meta*-position. That means the electron-donating character of the substituents has a more pronounced effect at the *ortho*- and

Table 3. Positional Effect of the R^1 Substituents on Seoul-Fluor



compd	R^1	σ	position	λ_{abs}^a	$\Delta(\text{eV})^b$	λ_{em}^c	Φ_{F}^d
SF25	CN		<i>ortho</i>	392	3.03	474	1.00
SF26	CN	0.56	<i>meta</i>	400	2.97	490	0.99
SF04	CN	0.66	<i>para</i>	407	2.96	494	0.99
SF27	Br		<i>ortho</i>	391	3.12	472	0.98
SF28	Br	0.39	<i>meta</i>	403	3.00	496	0.96
SF08	Br	0.23	<i>para</i>	405	2.98	502	0.90
SF29	OCH_3		<i>ortho</i>	405	3.01	503	0.82
SF30	OCH_3	0.12	<i>meta</i>	405	2.93	505	0.89
SF16	OCH_3	-0.27	<i>para</i>	412	2.84	526	0.69
SF31	$\text{N}(\text{CH}_3)_2$		<i>ortho</i>	410	2.86	548	0.51
SF32	$\text{N}(\text{CH}_3)_2$	-0.16	<i>meta</i>	408	2.74	529	0.30
E5	$\text{N}(\text{CH}_3)_2$	-0.83	<i>para</i>	440	2.56	613	0.15

^a Only the largest absorption maxima are shown. ^b Calculated value of the energy gap between the S_0 and S_1 states (see the Supporting Information). ^c Excited at the maximum absorption wavelength. ^d Absolute fluorescence quantum yield.

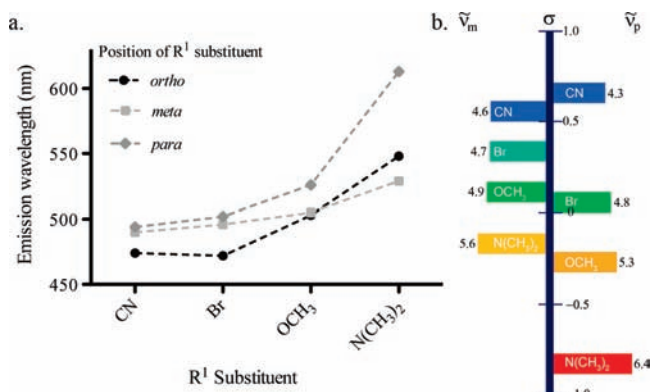
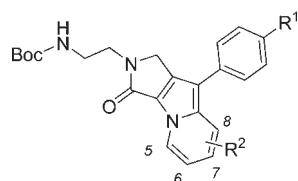


Figure 2. Positional effect of the R^1 substituent on the photophysical properties: (a) scatter plot of the emission wavelength of individual regioisomeric Seoul-Fluors with various R^1 substituents, (b) schematic representation of the Stokes shift (x axis) in wavenumbers (10^3 cm^{-1}) and Hammett constant σ (y axis) depending on the *meta* (σ_m , left side) and *para* (σ_p , right side) positions of the R^1 substituents.

para-positions than at the *meta*-position, which may imply a more drastic perturbation of the dipole moment at the *ortho*- and *para*-positions than that at the *meta*-position during an excited state based on the electronic character of the R^1 substituent.

As shown in Figure 2b, an increased Stokes shift was observed with an enhancement of the electron-donating character of the R^1 substituents, and these trends are more drastic at the *para*-position than at the *meta*-position. It is worth mentioning that the identical series of substituents (CN, Br, OCH_3 , and $\text{N}(\text{CH}_3)_2$) have a broader spectrum of electronic characters at the *para*-position than at the *meta*-position, which is in accordance with a larger change in σ_p than σ_m . In other words, more significant alterations in the electronic character of each R^1 substituent and

Table 4. Positional Effect of the R² Substituents on Seoul-Fluor

compd	R ¹	R ²	position	λ_{abs}^a	$\Delta(\text{eV})^b$	λ_{em}^c	Φ_{F}^d
SF33	Br	CH ₃	6	312	3.51	457	0.50
SF05	Br	CH ₃	7	318	3.48	462	0.33
SF34	Br	CH ₃	8	338	3.51	443	0.37
SF35	Br	COCH ₃	6	347	3.04	510	0.04
SF08	Br	COCH ₃	7	405	2.98	502	0.90
SF36	Br	COCH ₃	8	387	2.97	500	0.01
SF37	OCH ₃	CH ₃	6	344	3.41	472	0.47
SF13	OCH ₃	CH ₃	7	345	3.42	482	0.41
SF38	OCH ₃	CH ₃	8	339	3.60	459	0.73
SF39	OCH ₃	COCH ₃	6	354	2.93	537	0.03
SF16	OCH ₃	COCH ₃	7	412	2.84	526	0.69
SF40	OCH ₃	COCH ₃	8	340	2.89	526	0.01

^a Only the largest absorption maxima are shown. ^b Calculated value of the energy gap between the S₀ and S₁ states (see the Supporting Information). ^c Excited at the maximum absorption wavelength. ^d Absolute fluorescence quantum yield.

corresponding changes of the Stokes shift were observed at the *para*-position, as compared to the *meta*-position. On the basis of the fact that the expansion of the Stokes shift in wavelength reflects the increase in dipole moment at an excited state,²⁹ the *ortho*- and *para*-positions of the R¹ substituents on the phenyl ring are more suitable than the *meta*-position for an effective perturbation of the dipole moment and electronic status at an excited state, which can lead to dynamic changes in the emission wavelength.

Positional Effect of R² Substituents on the Photophysical Properties of Seoul-Fluor. We next focused on the positional effect of R² substituents and designed a synthetic route for a series of regioisomers at the R² position. In fact, there are several limitations for a robust introduction of R² substituents at various positions of Seoul-Fluor. First, the cycloaddition reaction, the key chemical transformation, did not proceed with the *ortho*-substituted pyridines. Therefore, variants of Seoul-Fluors with a substituent at the C-5 position were not synthetically feasible in this study. In contrast to the straightforward introduction of an R² group at the C-7 position using 4-substituted pyridine analogues, C-6 and C-8 regioisomers can be achieved through a synthesis with 3-substituted pyridine analogues and subsequent purification by preparative high-performance liquid chromatography. Variants of Seoul-Fluors with R² substituents at the C-7 position are synthetically more accessible than when other regioisomers are used, owing to their high yields and relatively easy purification.

In addition to the synthetic feasibility, 7-substituted Seoul-Fluor also demonstrated a noteworthy difference in its photophysical properties as compared to when 6- and 8-substituted regioisomers were used. As shown in Table 4, the aforementioned electronic effects of the R¹ groups on the photophysical properties were irrelevant to the position of the R² group; changes in the R¹ groups from EWG to EDG trigger a bathochromic shift regardless of the electronic states and positions of

the R² groups. For instance, a change in the R¹ groups from bromo (EWG) to methoxy (EDG) caused a 20 nm bathochromic shift in the emission wavelength on average, regardless of the position and electronic state of the R² groups. In addition, the electronic character of the R² groups influences the photophysical properties of all regioisomeric positions; a change in the R² groups from methyl (EDG) to acetyl (EWG) caused a bathochromic emission wavelength shift in all regioisomers. In other words, we did not observe significant differences in the emission wavelength upon positional changes of the R² groups in Seoul-Fluor, but we did observe a remarkable decrease in quantum yield by the introduction of an acetyl group at both the C-6 and C-8 positions. This tendency was orthogonal to the electronic property of the R¹ group, irrespective of it being an EWG (SF35, SF36) or an EDG (SF39, SF40). However, a decrease in quantum yield was not observed for the mild electron-donating methyl group introduced at the C-6 and C-8 positions; in fact, there was a slight increase in quantum yield in these cases. These observations are indicative of the positional effect of R² substituents on the photophysical properties of Seoul-Fluor via the resonance effect, not the inductive effect, which is an issue that remains to be addressed. Combining various observations, we concluded that the C-7 position of Seoul-Fluor is optimum for the introduction of various R² groups both synthetically and photophysically.

Predictability. After a systematic evaluation of the positional effects on the R¹ and R² substituents, we finalized the core structure of Seoul-Fluor using the R¹ substituents with phenyl group derivatives and the R² substituents at the C-7 position of the indolizine ring. On the basis of our previous observation of the significant correlation between the photophysical properties of Seoul-Fluor and the electronic characters of the substituents, we envisioned to extract the relationship between them. It is generally accepted that the absorption wavelength has high correlations with the calculated energy gap between the HOMO and LUMO,³⁰ but the emission wavelength has very little correlation with that due to the complex nature of the fluorescence process. Thus, the prediction of the emission wavelength, compared to absorption wavelength,³¹ in an organic fluorophore is extremely difficult and has not yet been achieved. However, this complexity in the prediction of the emission wavelength can be overcome through a systematic analysis of the emission wavelength of a single molecular framework, i.e., Seoul-Fluors, with various substituents. Therefore, we pursued a time-dependent density function theory (TD-DFT) calculation of the energy gaps between the ground state (S₀) and the first excited state (S₁) of the Seoul-Fluor variants synthesized in this study and compared this calculation with the emission wavelength of each variant. The calculations were executed with the optimized Cartesian coordinates using the Gaussian 03 program (B3LYP, 6-31G*; see the Supporting Information). As shown in Figure 3, we clearly observed an inverse linearity between the emission wavelength and the calculated energy gap of the Seoul-Fluor variants in a scatter plot. It is worth mentioning that emission wavelengths of 92% of the Seoul-Fluor variants were predicted with high accuracy (less than ± 30 nm error range) using a simple first-order equation without a sophisticated algorithm. We are confident that the emission wavelength can be predicted through a systematic analysis of a series of fluorophores in a single-core skeleton, because of a similar mechanism of non-radiative relaxation from an S₁ state as energy loss to the environment through vibration and/or rotation, a phenomenon found within an identical core skeleton.

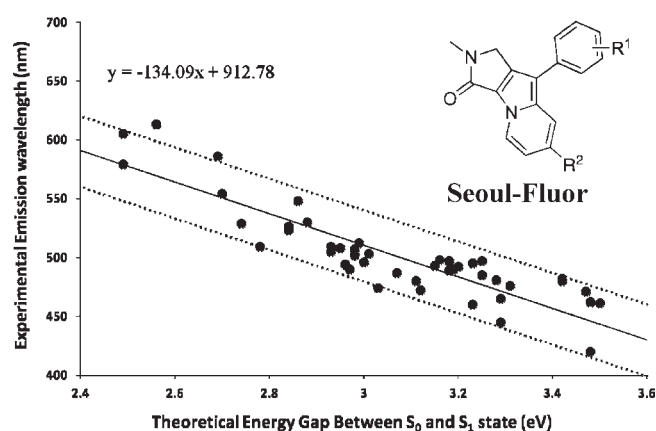


Figure 3. Scatter plot of Seoul-Fluor variants.

To confirm the usefulness of such predictability in our Seoul-Fluor system, covering the full color range, four different compounds were designed. For instance, to prepare blue emissive fluorescent compounds, CF_3 and a methyl group were selected as the R^1 and R^2 substituents, respectively, on the basis of theoretical calculation: the Hammett constant of the CF_3 substituent ($\sigma_p = 0.54$) is higher than that of Br (0.23) and lower than that of CN (0.66); therefore, the emission wavelength of SF41 was expected to be lower than 462 nm (SF05) and higher than 445 nm (SF01), indicating that a blue color emission should be expected. Using the same CF_3 substituent as in the R^1 group, changing the R^2 substituent from methyl (SF41) to acetyl (SF42) was expected to cause a 40–50 nm bathochromic shift, resulting in a green color emission, as shown in other cases in our system [for instance, changes in the substituent from SF01 (445 nm) to SF04 (494 nm) and SF09 (471 nm) to SF12 (509 nm), etc.]. Likewise, having changes in the R^1 substituent from SF42 to SF43 and to SF44, with lower Hammett constants following the sequence, three fluorophores with different colors were designed as a series of model compounds to confirm the predictability and the full-color coverage in the emission wavelengths of Seoul-Fluor (Figure 4).

After a careful but straightforward design, the emission wavelengths of model compounds were predicted using a first-order equation of the trend line, which we simply deduced from the fluorescent compound library. In agreement with our empirical expectation, energy gaps between the S_0 and S_1 states were predicted as 3.44, 3.03, 2.85, and 2.54 eV for SF41, SF42, SF43, and SF44, and the emission wavelengths were predicted as 451, 507, 531, and 573 nm for each compound, respectively. In the case of SF44, which contained a diethylamine group at the R^1 position, the emission wavelength was empirically expected to be 20–30 nm higher than the predicted value, as shown when other amine-containing compounds were used (for instance, SF20 and SF24). Therefore, we designed four different compounds that we predicted to cover the full color range with a 50 nm emission wavelength gap between each compound. Interestingly, the resulting experimental emission wavelengths of the designed compounds matched considerably well with the calculated value. For instance, the SF41, SF42, SF43, and SF44 compounds emit blue (450 nm), green (496 nm), yellow (530 nm), and red (611 nm) color emissions, respectively, and the average difference between their calculated emission values and experimental values

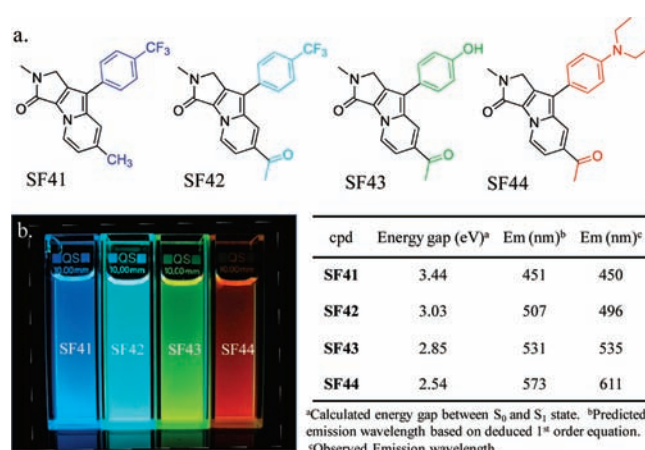


Figure 4. Practical predictability of Seoul-Fluor: (a) schematic illustration of the structure and color of each compound, (b) photographic image of the emission color of each compound, irradiated at 365 nm, and table of their photophysical properties.

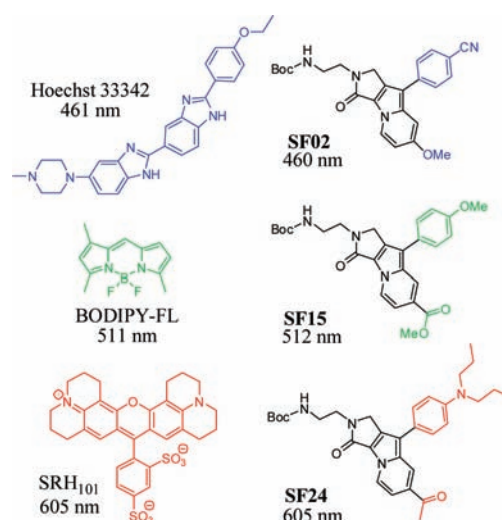


Figure 5. Comparison of common fluorescent dyes with Seoul-Fluor variants for their chemical structures and emission wavelengths.

was 14 nm. Therefore, from these observations, we confirmed that because the Seoul-Fluor system has a highly practical predictability, any of the desired fluorescent compounds within the full color range can be easily designed, and their photophysical properties can be predicted very simply.

CONCLUSION

A comparison of known fluorescent dyes extensively used in biological applications with Seoul-Fluors mirrored the unique features of our core skeleton. As shown in Figure 5, we used completely different structures of organic fluorophores to obtain a desired emission wavelength in biological experiments without considering that these structural differences might induce potential undesired interactions with various biopolymers. However, we can achieve the corresponding emission wavelengths of the known fluorescent dyes with Seoul-Fluors simply by changing the R^1 and R^2 substituents, which means that the desired

fluorescent compounds can be accessed using the Seoul-Fluor core skeleton with minimal structural perturbation.

Seoul-Fluor is a novel organic fluorophore with tunable emission wavelength covering the full range of visible color, which is particularly important from the perspective of multiplexing capability. In addition, a rational design, guided by systematic analysis, theoretical computation, and known numerical values, is possible with accurate and practical predictability; fluorescent compounds with desired photophysical properties can be acquired without the need for a tiresome synthesis and trial-and-error process. Therefore, this study revealed that we discovered a new fluorescent core skeleton, Seoul-Fluor, with full-color tunability and accurate predictability. Considering that the prediction of the emission wavelength of given fluorescent compounds is still rare and highly difficult, this remarkable result clearly shows how a combinatorial approach and systematic analysis can help us address these unsolved problems using a rational design-based approach and was exemplified with the development of novel organic fluorophores. With its unique properties, we hope that Seoul-Fluor can function as a versatile palette for developing desired fluorescent probes.

■ ASSOCIATED CONTENT

S Supporting Information. Detailed synthetic procedures, full characterization, and spectroscopic data of all new compounds, procedure and data of the computational study, and complete ref 3b. This material is available free of charge via the Internet at <http://pubs.acs.org>.

■ AUTHOR INFORMATION

Corresponding Author
sbpark@snu.ac.kr

■ ACKNOWLEDGMENT

This study was supported by the National Research Foundation of Korea (NRF) and the WCU program of the NRF funded by the Korean Ministry of Education, Science, and Technology (MEST). E.K., M.K., and B.J.L. are grateful for their predoctoral fellowships, awarded by the BK21 Program.

■ REFERENCES

- (1) (a) Lakowicz, J. R. *Principles of Fluorescence Spectroscopy*, 3rd ed.; Springer-Verlag: New York, 2006. (b) Rettig, W.; Strehmel, B.; Schrader, S.; Seifert, H., Eds. *Applied Fluorescence in Chemistry, Biology, and Medicine*; Springer: New York, 1999.
- (2) (a) Haugland, R. P. *Handbook of Fluorescence Probes and Research Products*, 10th ed.; Molecular Probes: Eugene, OR, 2005. (b) Lavigne, J. J.; Anslyn, E. V. *Angew. Chem., Int. Ed.* **2001**, *40*, 3118–3130. (c) Zhang, J.; Campbell, R. E.; Ting, A. Y.; Tsien, R. Y. *Nat. Rev. Mol. Cell. Biol.* **2002**, *3*, 906–918. (d) Domaille, D. W.; Que, E. L.; Chang, C. J. *Nat. Chem. Biol.* **2008**, *4*, 168–175.
- (3) (a) Goncalves, M. S. *Chem. Rev.* **2009**, *109*, 190–212. (b) Im, C.-N. et al. *Angew. Chem., Int. Ed.* **2010**, *49*, 7497–7500. (c) Urano, Y.; Asanuma, D.; Hama, Y.; Koyama, Y.; Barrett, T.; Kamiya, M.; Nagano, T.; Watanabe, T.; Hasegawa, A.; Choyke, P. L.; Kobayashi, H. *Nat. Med.* **2009**, *15*, 104–109.
- (4) (a) Tang, C. W.; Van Slyke, S. A. *Appl. Phys. Lett.* **1987**, *51*, 913–915. (b) Friend, R. H.; Gymer, R. W.; Holmes, A. B.; Burroughes, J. H.; Marks, R. N.; Raliani, C.; Bradley, D. D. C.; Dos Santos, D. A.; Brédas, J. L.; Lögdlund, M.; Salaneck, W. R. *Nature* **1999**, *397*, 121–128.

(c) Grimsdale, A. C.; Chan, K. L.; Martin, R. E.; Jokisz, P. G.; Holmes, A. B. *Chem. Rev.* **2009**, *109*, 897–1091.

- (5) Kim, E.; Park, S. B. *Chem.—Asian J.* **2009**, *4*, 1646–1658 and references therein.
- (6) Lavis, L. D.; Raines, R. T. *ACS Chem. Biol.* **2008**, *3*, 142–155.
- (7) Demchenko, A. P. *Advanced Fluorescence Reporters in Chemistry and Biology I*; Springer-Verlag: Berlin, Heidelberg, 2010; Chapter 2.5, pp 149–186.
- (8) Bruchez, M.; Moronne, M.; Gin, P.; Weiss, S.; Alivisatos, A. P. *Science* **1998**, *281*, 2013–2016.
- (9) Murray, C. B.; Norris, D. J.; Bawendi, M. G. *J. Am. Chem. Soc.* **1993**, *115*, 8706–8715.
- (10) Peng, Z. A.; Peng, X. *J. Am. Chem. Soc.* **2001**, *123*, 183–184.
- (11) Peng, Z. A.; Peng, X. *J. Am. Chem. Soc.* **2002**, *124*, 3343–3353.
- (12) Murray, C. B.; Kagan, C. R.; Bawendi, M. G. *Annu. Rev. Mater. Sci.* **2000**, *30*, 545–610.
- (13) Medintz, I. L.; Uyeda, H. T.; Goldman, E. R.; Mattoussi, H. *Nat. Mater.* **2005**, *4*, 435–446.
- (14) Michalet, X.; Pinaud, F. F.; Bentolila, L. A.; Tsay, J. M.; Doose, S.; Li, J. J.; Sundaresan, G.; Wu, A. M.; Gambhir, S. S.; Weiss, S. *Science* **2005**, *307*, 538–544.
- (15) Hardman, R. *Environ. Health Perspect.* **2006**, *114*, 165–172.
- (16) Duncan, T. V.; Park, S.-J. *J. Phys. Chem. B* **2009**, *113*, 13216–13221.
- (17) (a) Turro, M. J. *Modern Molecular Photochemistry*; University Science Books: Sausalito, CA, 1991. (b) Yang, T.; Goddard, J. D. *J. Phys. Chem. A* **2007**, *111*, 4489–4497.
- (18) (a) Vendrell, M.; Lee, J.-S.; Chang, Y.-T. *Curr. Opin. Chem. Biol.* **2010**, *14*, 383–389. (b) Finney, N. S. *Curr. Opin. Chem. Biol.* **2006**, *10*, 238–245.
- (19) Schidel, M.-S.; Briehn, C. A.; Bauërle, P. *Angew. Chem., Int. Ed.* **2001**, *40*, 4677–4680.
- (20) (a) Sivakumar, K.; Xie, F.; Cash, B. M.; Long, S.; Barnhill, H. N.; Wang, Q. *Org. Lett.* **2004**, *6*, 4603–4606. (b) Rosania, G. R.; Lee, J. W.; Ding, L.; Yoon, H. S.; Chang, Y.-T. *J. Am. Chem. Soc.* **2003**, *125*, 1130–1131. (c) Ahn, Y. H.; Lee, J. S.; Chang, Y.-T. *J. Am. Chem. Soc.* **2007**, *129*, 4510–4511. (d) Umezawa, K.; Nakamura, Y.; Makino, H.; Citterio, D.; Suzuki, K. *J. Am. Chem. Soc.* **2008**, *130*, 1550–1551. (e) Teo, Y. N.; Wilson, J. N.; Kool, E. T. *J. Am. Chem. Soc.* **2009**, *131*, 3923–3933.
- (21) Kim, E.; Koh, M.; Ryu, J.; Park, S. B. *J. Am. Chem. Soc.* **2008**, *130*, 12206–12207.
- (22) (a) Kim, J.; Song, H.; Park, S. B. *Eur. J. Org. Chem.* **2010**, 3815–3822. (b) Oh, S.; Nam, H. J.; Park, J.; Beak, S. H.; Park, S. B. *ChemMedChem* **2010**, *5*, 529–533. (c) Oh, S.; Jang, H. J.; Ko, S. K.; K, Y.; Park, S. B. *J. Comb. Chem.* **2010**, *12*, 548–558. (d) Kim, Y.; Kim, J.; Park, S. B. *Org. Lett.* **2009**, *11*, 17–20. (e) Park, S. O.; Kim, J.; Koh, M.; Park, S. B. *J. Comb. Chem.* **2009**, *11*, 315–326. (f) Lee, S.; Park, S. B. *Org. Lett.* **2009**, *11*, 5214–5217. (g) An, H.; Eum, S.-J.; Koh, M.; Lee, S. K.; Park, S. B. *J. Org. Chem.* **2008**, *73*, 1752–1761. (h) Lee, S.-C.; Park, S. B. *Chem. Commun.* **2007**, 3714–3716. (i) Ko, S. K.; Jang, H. J.; Kim, E.; Park, S. B. *Chem. Commun.* **2006**, 28, 2962–2964.
- (23) (a) *Clusters and Nanomaterials*; Kawazoe, Y., Ohno, K., Kondow, T., Eds.; Springer: New York, 2002. (b) Perdew, J. P.; Burke, K.; Ernzerhof, M. *Phys. Rev. Lett.* **1996**, *77*, 3865–3868. (c) Perdew, J. P.; Wang, Y. *Phys. Rev. B* **1996**, *45*, 13244–13249. (d) Kirkwood, J. C.; Scheurer, C.; Chernyak, V.; Mukamel, J. *J. Chem. Phys.* **2001**, *114*, 2419–2429. (e) Tretiak, S.; Chernyak, V.; Mukamel, S. *J. Phys. Chem. B* **1988**, *102*, 3310–3315. (f) Shimoi, Y.; Friedman, B. A. *Chem. Phys.* **1999**, *250*, 13–22.
- (24) Higashiguchi, K.; Matsuda, K.; Asano, Y.; Murakami, A.; Nakamura, S.; Irie, M. *Eur. J. Org. Chem.* **2005**, 91–97.
- (25) Melhuish, W. H. *J. Phys. Chem.* **1960**, *65*, 229–230.
- (26) Umberger, J. Q.; LaMer, V. K. *J. Am. Chem. Soc.* **1945**, *67*, 1099–1109.
- (27) Magde, D.; Brannon, J. H.; Cremers, T. L.; Olmsted, J., III. *J. Phys. Chem.* **1979**, *83*, 696–699.
- (28) Hansch, C.; Leo, A.; Taft, R. W. *Chem. Rev.* **1991**, *91*, 165–195.

(29) Reichards, C. *Solvents and Solvent Effects in Organic Chemistry*, 3rd ed.; Wiley-VCH: Weinheim, Germany, 2003.

(30) Patalinghug, W. C.; Chang, M.; Solis, J. J. *Chem. Educ.* **2007**, *84*, 1945–1947.

(31) (a) Zollinger, H. *Color Chemistry*; VCH: Weinheim, Germany, 1991; see also references therein. (b) Bauernschmitt, R.; Ahlrichs, R.; Hennrich, F. H.; Kappes, M. M. *J. Am. Chem. Soc.* **1998**, *120*, 5052–5059.